

## Linear *dsDNA* Partitions Spontaneously into the Inverse Hexagonal Lyotropic Liquid Crystalline Phases of Phospholipids

Camilla F. Black,<sup>†</sup> Richard J. Wilson,<sup>†</sup> Tommy Nylander,<sup>‡</sup> Marcus K. Dymond,<sup>†</sup> and George S. Attard<sup>\*†</sup>

*School of Chemistry, University of Southampton, Southampton, SO17 1BJ, United Kingdom, and Physical Chemistry 1, Center for Chemistry and Chemical Engineering, Lund University, P.O. Box 124, SE-221 00 Lund, Sweden*

Received February 23, 2010; E-mail: gza@soton.ac.uk

**Abstract:** Recently, we reported that DNA associated with inverse hexagonal ( $H_{II}$ ) lyotropic liquid crystal phases of the lipid 1,2-dioleoyl-*sn*-glycero-3-phosphoethanolamine (DOPE) was actively transcribed by T7 RNA polymerase.<sup>1</sup> Our findings suggested that key components of the transcription process, probably the T7 RNA polymerase and the DNA, remained associated with the monolithic  $H_{II}$  phase throughout transcription. Here, we investigate the partitioning of DNA between an  $H_{II}$  lyotropic liquid crystal phase and an isotropic supernatant phase in order to develop insights into the localization of DNA in liquid crystalline environments. Our results show that linear double stranded DNA (*dsDNA*) molecules partition spontaneously into monolithic preformed  $H_{II}$  liquid crystal phases of DOPE. We propose that this process is driven by the increase in entropy due to the release of counterions from the DNA when it inserts into the aqueous pores of the  $H_{II}$  phase.

### Introduction

Assemblies of double stranded DNA (*dsDNA*) with lipids and surfactants are well reviewed in the literature;<sup>2</sup> the type of assemblies that are formed range from DNA molecules compacted around vesicles through to normal topology hexagonal ( $H_I$ ),<sup>3</sup> lamellar ( $L_\alpha$ ),<sup>4</sup> and inverse hexagonal ( $H_{II}$ )<sup>5</sup> lyotropic liquid crystal phases where the DNA resides within the aqueous domain of the phase, stabilized by electrostatic lipid headgroup/DNA interactions. The majority of DNA–lipid assemblies that have been reported are particulate in nature, which is a consequence of their formation by precipitation following self-organization from relatively dilute solutions of the components. It is generally accepted<sup>6</sup> that the primary drive for the interaction of DNA with the surfaces of lipid vesicles is entropic, resulting from the release of cations bound to the anionic DNA macromolecule. Particulate complexes having a lamellar nanoarchitecture, resulting from mixing vesicles containing cationic

lipids with solutions of DNA, were some of the earliest systems studied. These complexes, which are often referred to as lipoplexes, are of continuing interest because of their potential use as delivery systems for gene transfection. The presence of cationic lipids is not essential for the formation of lipoplexes as it has been shown that DNA will form complexes, with an  $H_{II}$  nanoarchitecture, with zwitterionic lipids such as 1,2-dioleoyl-*sn*-glycero-3-phosphoethanolamine (DOPE)<sup>7</sup> in the presence of divalent cations like  $Mg^{2+}$ . DNA also forms complexes with anionic liposomes<sup>8</sup> in the presence of calcium; this is because divalent cations are able to bridge between the anionic phosphate groups of the DNA molecule and the anionic head groups of the lipids.<sup>9</sup> In the case of zwitterionic phospholipids, divalent cations are thought to favor the formation of lipoplexes by bridging the phosphate groups of neighboring lipid molecules to leave a net positive charge on the surface of the lipid aggregate.

The self-organized nanoarchitectures of the particles that are obtained when DNA is mixed with lipids or other surfactants are dependent on the structural parameters of the lipids and surfactants used and on their relative concentrations. The nanoarchitecture of a lipid aggregate is determined by the mean ( $\kappa_M$ ) and Gaussian ( $\kappa_G$ ) curvature elastic moduli of the lipid components and their overall spontaneous curvature ( $c_o$ ). Broadly speaking, these translate into shape (steric) factors and headgroup–headgroup interactions.<sup>5</sup> Thus, to a first approxima-

<sup>†</sup> University of Southampton.

<sup>‡</sup> Lund University.

- (1) Corsi, J.; Dymond, M. K.; Ces, O.; Muck, J.; Zink, D.; Attard, G. S. *Chem. Commun.* **2008**, 2307–2309.
- (2) Dias, R. S.; Dawson, K.; Miguel, M. G. In *DNA Interactions with Polymers and Surfactants*; Dias, R. S., Lindman, B., Eds.; John Wiley and Sons: Hoboken, NJ, 2008; pp 89–117.
- (3) Leal, C.; Wadsoe, L.; Olofsson, G.; Miguel, M.; Wennerström, H. J. *Phys. Chem. B* **2004**, *108*, 3044–3050.
- (4) Radler, J. O.; Koltover, I.; Salditt, T.; Safinya, C. R. *Science* **1997**, *275*, 810–814.
- (5) Koltover, I.; Salditt, T.; Radler, J. O.; Safinya, C. R. *Science* **1998**, *281*, 78–81.
- (6) Podgornik, R.; Harries, D.; DeRouchey, J.; Strey, H. H.; Parsegian, V. A. In *Gene Therapy: Therapeutic Mechanisms and Strategies*, 3rd ed.; Smythe-Templeton, N., Ed.; Marcel Dekker: New York, 2008; pp 443–484.

(7) Francescangeli, O.; Pisani, M.; Stanic, V.; Bruni, P.; Weiss, T. M. *Europhys. Lett.* **2004**, *67*, 669–675.

(8) Patil, S. D.; Rhodes, D. G.; Burgess, D. J. *AAPS J.* **2004**, *6*, e29.

(9) Mengistu, D. H.; Bohinc, K.; May, S. J. *Phys. Chem. B* **2009**, *113*, 12277–12282.

tion,<sup>10</sup> double-hydrocarbon chain molecules with smaller head groups (type II lipids) favor the formation of inverse topology aggregates (e.g., inverse micelles,  $H_{II}$  and inverse bicontinuous cubic phases), while single chain molecules with larger head groups (type I lipids) favor normal topology aggregates (e.g., micelles,  $H_I$ , and cubic phases). When the sizes of the headgroup and hydrocarbon chain cross sections are similar (type 0 lipids), bilayer aggregates like liposomes and lamellar phases are favored. Equally, lipid mixtures in which there are strong inter-headgroup interactions (e.g., fatty acid–phosphatidylcholine mixtures) will favor inverse topology architectures.<sup>11</sup>

Recently, we discovered that dsDNA 4331 bp in length, which was prepared as a monolithic single-phase mixture with the ( $H_{II}$ ) lyotropic liquid crystal phase of the lipid DOPE, was actively transcribed by T7 RNA polymerase.<sup>1</sup> In our previous study, the DNA was incorporated into the liquid crystal phase by micro-mixing *lin-pT7luc* with DOPE and forming the  $H_{II}$  phase by using a 0.15 M saline solution to hydrate the lipid/DNA mixture. Under these conditions, we were able to demonstrate that while the DNA was accessible to the T7 RNA polymerase, no significant transcription was occurring in solution. While our initial observations suggested that the DNA remained associated with the monolithic  $H_{II}$  phase throughout transcription, the positioning of the DNA in relation to the architecture of the inverse hexagonal phase remained unresolved. Here, we describe our studies of solutions of double stranded DNA in contact with preformed monolithic  $H_{II}$  lyotropic liquid crystal phases, and show that the DNA molecules are absorbed spontaneously into the aqueous channels of the  $H_{II}$  phase and that the adsorption of the dsDNA results in a swelling of the unit cell of the  $H_{II}$  phase.

## Results and Discussion

The basis for the determination of the partition coefficient of a linear strand of dsDNA is a new experimental technique that makes use of PCR to amplify DNA that is present in a supernatant solution in contact with the monolithic  $H_{II}$  phase. The concentration of the PCR product is quantified spectrophotometrically, and is then converted to an estimate of the concentration of the DNA taken from the supernatant by using a calibration curve showing the amplification for different concentrations of template DNA. Figure 1 shows the standard curve used to quantify the amount of supernatant *lin-T7gfp* DNA. The amplification factor (defined as the ratio of the amount of PCR product to the amount PCR template) has a power-law dependence on the amount of PCR template, with an exponent of  $-1.24 \pm 0.03$ , which means that this technique is particularly sensitive at the lower template concentrations used in this study.

Since the standard process we developed for preparing the DNA-containing lipid buttons involves a freeze-drying step, it is likely that, following lyophilization, some or all of the DNA may form a compacted mass on the external surface of the lipid button. Upon hydration of the mixture with saline, the lipid will form an  $H_{II}$  phase rapidly. By contrast, the DNA will take longer to hydrate, particularly if it is partially crystallized. Consequently, upon addition of the supernatant phase, the dynamics of the redistribution of the DNA to achieve the equilibrium amounts in supernatant and liquid crystalline phase are expected

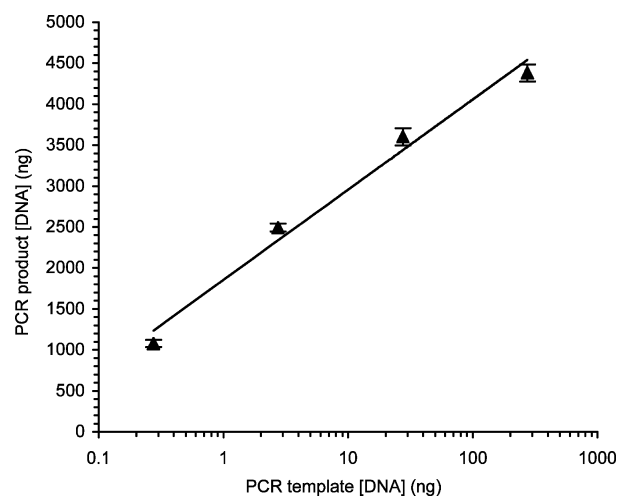


**Figure 1.** Calibration curve for *lin-pT7gfp* DNA which shows the change in the amount of PCR product as a function of the amount of template DNA used. It is noted that the amplification factor,  $A$ , increases as  $T^{-1.24}$ , as the concentration of template DNA ( $T$ ) decreases. Because of small variations in the PCR process that are outside of our control, we found that the most accurate results were obtained when the calibration curve was obtained in the same PCR runs that were used to quantify the amount of DNA in the supernatant.

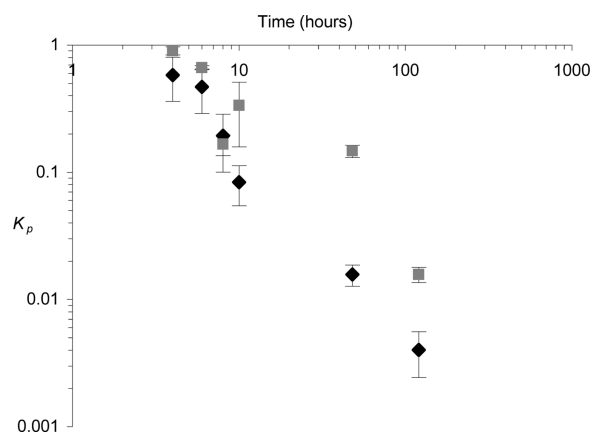


**Figure 2.** Relationship between the partition coefficient for *lin-pT7gfp* DNA and the time of incubation at 37 °C. Diamonds depict the partition coefficients obtained from experiments in which the DNA was mixed with the lipid via lyophilization. Squares show the partition coefficients from experiments in which the DNA is initially added to the supernatant liquid above the  $H_{II}$  phase (i.e.,  $K_p = 1$ ).

to be complex and possibly very slow. To overcome this problem, an alternative set of samples was set up in which the hydrated  $H_{II}$  phases were placed in contact with solutions of the DNA. In these systems, the equilibrium composition of the supernatant and  $H_{II}$  phases should be the same as for the lyophilized samples. The partition coefficients obtained from these two methods for different incubation times are plotted in Figure 2.

The data suggest that the equilibrium partition coefficient is  $\leq 8 \times 10^{-3}$ , indicating that the *lin-pT7gfp* DNA has a strong preference to partition into the liquid crystalline phase. It is interesting to note that this value of the equilibrium constant is approached over a period of around 100 h. The plots also show that the equilibration of the system in which the DNA is initially all present in the supernatant is slower than for the system in which the DNA is lyophilized.

The data presented in Figure 2 indicate that the most likely location of the DNA at equilibrium is within the pores of the

(10) Dymond, M.; Attard, G.; Postle, A. D. *J. R. Soc. Interface* **2008**, *5*, 1371–1386.

(11) Seddon, J. M. *Biochim. Biophys. Acta* **1990**, *1031*, 1–69.

$H_{II}$  phase. This is consistent with the structure of the  $H_{II}$  phase of DOPE, which has cylindrical pores with diameter of 4 nm<sup>12</sup> that can accommodate a DNA helix in the B form, which has a diameter of  $\sim 2$  nm. It is also consistent with small-angle X-ray diffraction data from complexes obtained by mixing DOPE/DOTAP binary liposomes with  $\lambda$ -phage DNA in deionized water. Although these complexes differ from our systems in that they are particulate with an average size of 0.2  $\mu\text{m}$  and are formed in the absence of salts or divalent cations, they show that dsDNA can be accommodated inside the aqueous pores of a homogeneous hexagonal phase ( $H_{II}^C$ ) for mixtures with a DOPE weight fraction between 0.7 and 0.85.<sup>13</sup> The supposition that at equilibrium the system in our partition experiments consists of DNA inside the pores of the liquid crystalline phase is also consistent with a report<sup>7</sup> that  $H_{II}$  lipoplexes of DNA and DOPE lipids form spontaneously from aqueous solutions of DOPE and DNA in the presence of divalent cations ( $\text{Mg}^{2+}$ , in this system). The limiting partition coefficient ( $2 \times 10^{-2}$  to  $8 \times 10^{-3}$ ) that we observe after 100 h equilibration corresponds to an equilibrium constant for the partition process of 49–124, which gives a free energy of  $-9.6$  to  $-12.4$  kJ mol<sup>-1</sup>, indicating a strong drive to partition.

The localization of the DNA in the pores is also implied by an estimate of the amount of DNA that can be packed on the surface of a lipid button. The 2 mg lipid buttons have an approximate hemispherical shape with a radius of  $\sim 1.5 \times 10^{-3}$  m. The surface area that may be accessible to the supernatant solution ranges from  $\sim 7.1 \times 10^{-6}$  m<sup>2</sup> (for the top surface) to  $14 \times 10^{-6}$  m<sup>2</sup> (this allows for the supernatant to seep between the wall of the PCR tube and the button such that the entire surface of the lipid button is in contact with the supernatant). It is noted that these estimates are based on the assumption that the surface of the lipid monolith is smooth. The length of a fully extended molecule of *lin-pT7gfp* (3395 bp) is estimated to be  $1.2 \times 10^{-6}$  m. Assuming that the DNA helix is in the B form means that the DNA can be represented as a cylinder with a radius  $10 \times 10^{-10}$  m. We can now distinguish between two possibilities: either the DNA molecules partition flat on the external surface of the lipid button, or they are inserted into the 4 nm diameter aqueous pores of the  $H_{II}$  phase. In the case of DNA molecules lying flat on the external surface, the longitudinal cross section ( $2.4 \times 10^{-16}$  m<sup>2</sup> per molecule) of an extended DNA 'rod' enables us to estimate the maximum number of DNA molecules that could be packed as a monolayer; this is in the range of  $1.5 \times 10^9$  to  $3 \times 10^9$  molecules. The RMM of *lin-pT7gfp* is estimated to be  $\sim 2.21 \times 10^6$  g mol<sup>-1</sup> (by using an average base pair RMM of 652 g mol<sup>-1</sup>), so the 1  $\mu\text{g}$  of DNA used in our studies corresponds to  $\sim 2.7 \times 10^{11}$  molecules of DNA per lipid button. If all these DNA molecules were located flat at the surface, then about 90–180 stacked monolayers would be required to remove all DNA from solution. DNA aggregation at this level would only be explicable through insolubility or colloidal coagulation. In the case where the DNA molecules insert into the aqueous pores of the phase, the number of aqueous pores in contact with the supernatant is estimated to be in the range of  $1.5 \times 10^{11}$  to  $3 \times 10^{11}$ . This estimate uses the unit cell dimension ( $d$ ) of  $H_{II}$ -DOPE at 37 °C in water ( $7.0 \pm 0.4 \times 10^{-9}$  m) obtained from small-angle X-ray diffraction, to calculate the number of pores per unit area of surface ( $\sim 44$  nm<sup>-2</sup>). Since the number of  $H_{II}$  phase aqueous pores in contact with the supernatant phase is estimated to be of the order of

$10^{11}$ , it is possible for all the molecules of DNA (also of the order of  $10^{11}$  molecules) to partition into the phase, even for the limiting case of only one DNA molecule per pore. Calculations for *lin-pT7luc* DNA, which is 4331 bp long, lead to very similar estimates. It is noted that the monolithic buttons used in these studies are macroscopically unoriented; that is, they are polydomain samples in which the typical size of the domains having orientational coherence appears to be ca. 10  $\mu\text{m}$  as judged by polarized light microscopy. The polydomain nature of the samples means that the pore system of the  $H_{II}$  phase will have a range of orientations relative to the sample surface. The direct interaction of DOPE molecules or aggregates in solution with the dsDNA can be discounted on two grounds. First, the critical aggregation of DOPE is  $< 10^{-12}$  M; hence, the concentration of DOPE monomers in solution is insufficient to drive a process of DNA precipitation onto the surface that removes 1  $\mu\text{g}$  of DNA. Second, we have found no evidence of vesicle or particulate detachment from the surface when the  $H_{II}$  phase is brought in contact with a DNA solution. Taken together, our order of magnitude estimates and our observations of the partition coefficients suggest that it is highly likely that linear dsDNA partitions into the pores of the  $H_{II}$  phase of the DOPE lipid button, but that the equilibration process occurs relatively slowly.

Throughout this discussion, we have assumed that the dsDNA is in the B-form, which is postulated to be one of the two canonical forms that occur *in vivo*. A recent structural analysis of calf thymus dsDNA complexed with a range of lipids and amphiphiles in Tris buffer suggests that the conformation of the DNA within a complex depends on the nature of the lipids present.<sup>14</sup> Of particular relevance to our study is the observation that when mixed with DOPE the DNA shows a partial B form to A form transition. From X-ray diffraction studies, it is known that the aqueous pores in the  $H_{II}$  phase of DOPE have diameters of ca. 4.0 nm at 37 °C,<sup>12</sup> and hence are able to accommodate either form of the DNA. Furthermore, it is well-known that elevated ionic strength, di- or multivalent counterions, and reduced water activity favor the Z-form of DNA.<sup>15</sup> Since our DNA–DOPE mixtures are prepared in buffer and contain a significant concentration of magnesium ions ( $25 \times 10^{-3}$  M), it is also possible that the DNA that is associated with the  $H_{II}$  phase may be in the Z form. Unfortunately, due to the highly scattering nature of the liquid crystalline phase and its birefringence, it is not possible to employ CD or IR techniques to determine the structure of the DNA and the precise structure of the DNA that is associated with the liquid crystalline phase remains a matter of conjecture.

A further piece of evidence that DNA does indeed penetrate into the preformed pores of  $H_{II}$  phases comes from time-lapse fluorescence imaging microscopy of the partitioning process, shown in Figure 3, where a solution of *lin-pT7luc* is brought into contact with the  $H_{II}$  phase of DOPE that has been loaded with propidium iodide.

Because of constraints of scale, it is impossible to reproduce precisely the same conditions that were used in the partitioning experiments (i.e., lipid to DNA ratios). While the amount of lipid used in the fluorescence studies is similar to that used in the partitioning experiments, the  $H_{II}$  phase surface area that is

(12) Tate, M. W.; Gruner, S. M. *Biochemistry* **1989**, *28*, 4245–4253.

(13) Safinya, C. R. *Curr. Opin. Struct. Biol.* **2001**, *11*, 440–448.

(14) Marty, R.; N'soukpoé-Kossi, C. N.; Charbonneau, D.; Weinert, C. M.; Kreplak, L.; Tajmir-Riahi, H. A. *Nucleic Acids Res.* **2009**, *37*, 849–857.

(15) Jovin, M. T.; Soumpasis, D. M. *Annu. Rev. Phys. Chem.* **1987**, *38*, 521–560.



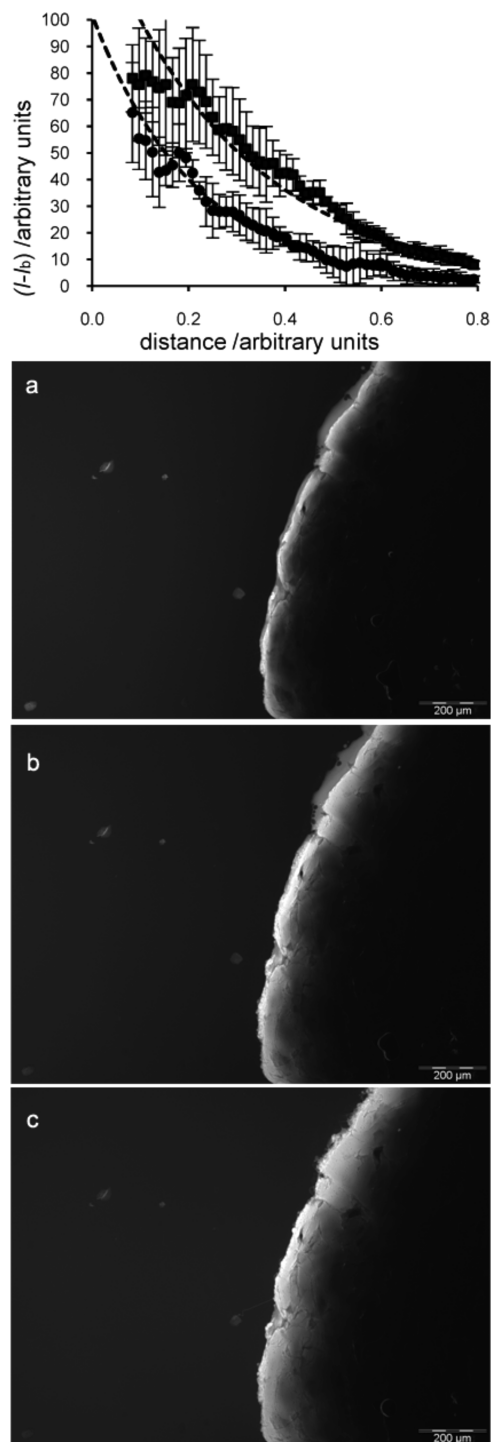


**Figure 3.** Time-lapse fluorescence microscopy study showing the penetration of dsDNA into a thin layer ( $\sim 100 \mu\text{m}$  thick)  $H_{II}$  phase of DOPE sandwiched between a microscope slide and coverslip. (a) The  $H_{II}$  phase in excess buffer containing propidium iodide without DNA. The bright edge of the sample with no DNA arises from fluorescence due to local enrichment of propidium iodide at the phase surface and the effect of light focusing by the phase edge. (b) The same system 5 min and (c) 15 min after the addition of *lin-pT7luc* DNA. The increase in fluorescence intensity arises as a result of propidium iodide binding to the DNA, which then penetrates into the  $H_{II}$  phase as illustrated by the average intensity profiles, in which background fluorescence has been subtracted, that are shown in the top figure. The lower of the two curves is the average intensity profile across the interface for image (b), while the upper of the curves is for image (c).

in contact with the DNA solution is much reduced, and the DNA concentrations used are almost an order of magnitude larger.

However, the sequence of micrographs shows clearly that the DNA penetrates into  $H_{II}$  phase to a depth of approximately  $100 \mu\text{m}$ . This study also shows that both the position of the sample interface and the surface smoothness of the monolithic  $H_{II}$  phase do not change significantly upon addition of the DNA.

The final piece of evidence to support the partitioning of dsDNA inside the channels of the  $H_{II}$  phase is provided by small-angle X-ray diffraction measurements of monolithic DOPE  $H_{II}$  phases incubated with solutions of dsDNA. We observed  $H_{II}$  phases with unit cell dimensions ( $d$ ) of  $7.40 \times 10^{-9} \text{ m}$  (DOPE with Salmon sperm DNA and  $25 \text{ mM Mg}^{2+}$ ),  $7.26 \times 10^{-9} \text{ m}$  (DOPE with Salmon sperm DNA and no  $\text{Mg}^{2+}$ ), and  $7.40 \times 10^{-9} \text{ m}$  (DOPE with *lin-pT7gfp* and transcription mixture containing  $25 \text{ mM Mg}^{2+}$ ), compared with  $7.04 \times 10^{-9} \text{ m}$  for DOPE in excess water and  $5.76 \times 10^{-9} \text{ m}$  for DOPE in excess water containing  $25 \text{ mM Mg}^{2+}$ . Hence, in the presence of  $25 \text{ mM Mg}^{2+}$  ions, the unit cell dimension of the  $H_{II}$  phase is reduced significantly from its value in pure water. This is analogous to the situation reported for the effect of  $\text{Mn}^{2+}$  ions on the lamellar spacing in the  $L_{\alpha}$  phase of DOPC<sup>7</sup> and consistent with the divalent ions bridging neighboring headgroups and causing a contraction in the inter-headgroup separation. However, upon addition of dsDNA, the phase swells such that the unit cell dimension of the phase is bigger than for the  $H_{II}$  phase of DOPE and water. We note that this is the case irrespective of whether the system contains  $\text{Mg}^{2+}$  ions. It is instructive to compare our data with the results reported by Koltover et al.<sup>5</sup> for DOPE/DOTAP/ $\lambda$ -phage DNA mixtures. In these systems, which are produced as fine precipitates at room temperature and in the absence of divalent cations, the presence of 0.3–0.15 weight fraction of DOTAP stabilizes an  $H_{II}^C$  phase in which  $d$  varies linearly from 6.7 to  $6.9 \times 10^{-9} \text{ m}$  as the weight ratio of DOTAP decreases. The unit cell spacing for a  $H_{II}^C$  phase comprising only DOPE and DNA (i.e., no DOTAP) can be estimated by extrapolation to be  $\sim 7.2 \times 10^{-9} \text{ m}$ . We note that the value of  $d$  for the  $H_{II}$  phase of DOPE in water is quoted as  $7.4 \times 10^{-9} \text{ m}$  and so the  $H_{II}^C$  phase appears to have a unit cell dimension that is consistently less than the  $H_{II}$  phase of pure DOPE. By contrast, in our dsDNA/ $H_{II}$ -DOPE systems, the unit cell dimensions are consistently larger than for the phase of pure DOPE. This observation raises the possibility that the  $H_{II}^C$  phase obtained by precipitation may not be an equilibrium structure.

Having found experimentally that long molecules of dsDNA partition spontaneously into the aqueous pores of the  $H_{II}$  phase of DOPE, the question arises as to underlying physical interactions that drive this process. Studies on the condensation of dsDNA-surfactant systems together with studies on the adsorption of dsDNA on a variety of surfaces have established that the interaction of the negatively charged DNA with positively charged surfaces results in the release of monovalent counterions from the DNA, providing a strong entropic drive for condensation/adsorption. In solution, dsDNA is a stiff random coil with a persistence length of around  $5 \times 10^{-8} \text{ m}$ ,<sup>16</sup> and contains cations bound to the phosphate groups of its backbone, thereby neutralizing their negative charge. Insertion of the DNA into the 4 nm wide aqueous channels of the  $H_{II}$  phase would lead to a loss of conformational entropy, which would disfavor partitioning into the phase. However, insertion of DNA would also lead to an increase in the configurational entropy of the system through the release of monovalent counterions and

(16) Maret, G.; Weill, G. *Biopolymers* **1983**, *22*, 2727–2744.

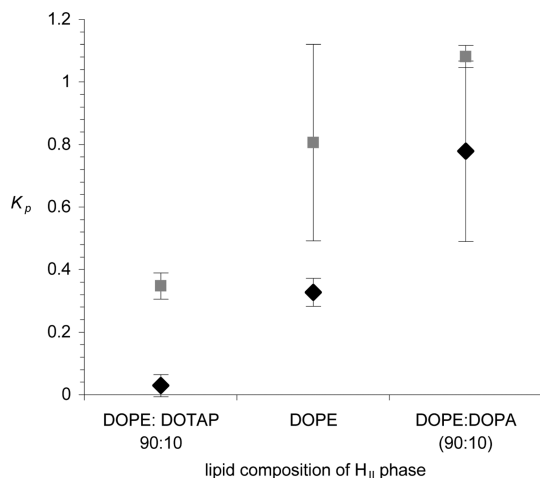


**Figure 4.** The influence of charged lipids on the partitioning of DNA into the  $H_{II}$  phases of lipids. Diamonds represent lipid buttons prepared by lyophilization; squares show experiments in which the DNA is initially added to the supernatant liquid above the  $H_{II}$  phase. Data are for *lin-pT7gfp* and for a total incubation time of 14 h.

displacement of counteranions from the  $H_{II}$  pore upon DNA insertion. The presence of  $Mg^{2+}$  ions in the transcription buffer leads to the internal surfaces of the  $H_{II}$  phase of DOPE acquiring an overall positive charge because the  $Mg^{2+}$  ions bridge the negatively charged phosphate moieties in adjacent lipid head groups. This surface charge is balanced by counteranions (mostly  $Cl^-$ ) within the pore volume. Insertion of DNA displaces these counteranions and at the same time counterions in the DNA (mostly  $Na^+$ ) are exchanged for the lipid surface charges, and so are released into solution increasing the configurational entropy of the system. In theory, a maximum of  $6.79 \times 10^3$   $Na^+$  ions could be released per inserted DNA molecule, with an equivalent number of monovalent anions.

According to our analysis, the driving force for the partitioning of *dsDNA* into the aqueous pores of the  $H_{II}$  phase is an increase in the configurational entropy that results from changes in electrostatic interactions upon insertion of the DNA in the pores of the phase. On the basis of this behavior, it follows that doping the DOPE  $H_{II}$  phase with the cationic lipid DOTAP should increase the amount of DNA taken up by the phase (i.e., decreases the partition coefficient), while doping the phase with the anionic lipid DOPA would decrease the amount of DNA taken up (i.e., increases the value of the partition coefficient). The experimental data shown in Figure 4, which summarizes

the magnitudes of the partition coefficients after 14 h incubation, are consistent with these predictions.

## Conclusions

Our observation that *dsDNA* spontaneously partitions into the  $H_{II}$  phases of phospholipids under the conditions that were used to transcribe this DNA raises the possibility that, *in vivo*, the genome interacts with endonuclear lipids to form a self-organized nanoarchitecture. If this is the case, then it is possible that transcription, and maybe other genome processes, may occur within a structured environment, or conversely, that the nanoarchitecture of the nuclear matrix may influence genome processes. The organization of genomic DNA into liquid crystalline phases has been reported previously; small-angle X-ray diffraction studies on *Escherichia coli* JM109 cells that carry a high copy number of non-nucleosomal Blue Script plasmid show Bragg peaks at 49.1 and 51.5 Å, attributed to a columnar lyotropic phase occurring due to the high volume fraction of plasmid DNA.<sup>17</sup> In addition, *in vivo*, the highly condensed DNA of the dinoflagellate *Prorocentrum micans*<sup>18</sup> reportedly forms liquid crystal phases. Our findings provide an insight into the self-organizational behavior of DNA and phospholipids that may form part of the mechanism of the transcription process *in vivo*. The thermodynamic stability of DNA within the aqueous channels of the  $H_{II}$  phases coupled with its potential accessibility to the transcription machinery of eukaryotes may also inform the interpretation of transfection efficiency data for lipoplex systems. Furthermore, the kinetics of DNA insertion into the nanochannels of the liquid crystalline phase may have implications for emerging technologies that are based on the use of nanopores for DNA sequencing.<sup>19–20</sup>

**Acknowledgment.** The authors would like thank Daniele Zink for suggesting the experiment, Ali Tavassoli for guidance in the design of their PCR experiments and use of his laboratory facilities for the proof-of-concept experiments, Josephine Corsi for contributing with her experience in transcription of DNA associated with the  $H_{II}$  lyotropic liquid crystal phases and members of the Neonuclei consortium for critical appraisal of the work. We also would like to thank the I711 beamline team at MAX-lab for beam-time allocation, and in particular Tomás Plivelic and Yngve Cerenius for generous help and discussions. This work was supported by the European Union FP6 framework under the project title of Neonuclei, project number 12967.

**Supporting Information Available:** Full experimental details for the processes of monolithic  $H_{II}$  phase preparation, plasmid preparation and linearization, quantification of *dsDNA* by PCR amplification, partition coefficient calculation, fluorescence microscopy and X-ray diffraction. This material is available free of charge via the Internet at <http://pubs.acs.org>.

JA101550C

(17) Reich, Z.; Wachtel, E.; Minsky, A. *Science* **1994**, *264*, 1460–1463.

(18) Livolant, F.; Maestre, M. F. *Biochemistry* **1988**, *27*, 3056–3068.

(19) Ashkenasy, N.; Sánchez-Quesada, J.; Bayley, H.; Ghadiri, M. R. *Angew. Chem., Int. Ed.* **2005**, *44*, 1401–1404.

(20) Kasianowicz, J. J.; Brandin, E.; Branton, D.; Deamer, D. W. *Proc. Natl. Acad. Sci. U.S.A.* **1996**, *93*, 13770–13773.